2.4 Steady flow from a deep reservoir.

Following discussions with H. Stommel in the early 1970s, Whitehead, Leetma and Knox (1974), hereafter WLK, developed the first analytical model of hydraulic behavior in a steady, rotating-channel flow with topography. Their model utilizes rectangular cross-sectional geometry and is based on the zero potential vorticity limit [$q \to 0$ with w=O(1)]. Since $q=D/D_\infty$ and $w=w^*f/(gD)^{1/2}$, the channel width is comparable to the Rossby deformation radius based on the local depth scale D, while D itself is much less than the potential depth. The situation envisioned by WLK is that the flow is fed from a reservoir that is deep and quiescent, and in which the layer thickness is therefore D_∞. Fluid is drawn up from a reservoir and over a relatively shallow sill, where the depth scale $D<<D_\infty$.[1] With q=0 the absolute vorticity of the fluid is zero ($\partial v/\partial x + 1 = 0$) and the depth profiles are given by (2.2.29) for attached flow and (2.3.14) for separated flow. These profiles are valid only as long as the local depth remains much smaller than the reservoir depth. The calculation therefore cannot be extended indefinitely far upstream from the shallow section of channel.

For the case of attached flow, y-variations of the current are governed by the steady versions of (2.2.15) and (2.2.16), which express conservation of the volume flow rate Q and average $\overline{B}$ of the sidewall Bernoulli functions. The flow rate is defined in terms of average $(\overline{d})$ and difference $(\hat{d})$ of the wall depths by

$$Q = 2\hat{d}\overline{d}\,. \tag{2.4.1}$$

In the limit $q \to 0$, the average Bernoulli function (2.2.17) is

$$\overline{B} = \frac{2\hat{d}^2}{w^2} + \frac{w^2}{8} + \overline{d} + h\,. \tag{2.4.2}$$

Elimination of $\hat{d}$ between the last two relations yields

$$\frac{Q^2}{2\overline{d}^2 w^2} + \frac{w^2}{8} + \overline{d} + h - \overline{B} = 0\ , \tag{2.4.3}$$

which is of the form of the standard hydraulic relation $\mathcal{G}(\overline{d}; w, h; Q, \overline{B}) = 0$ sought by Gill(1977). Here $\overline{d}$ represents the single variable characterizing the flow cross-section; if $\overline{d}$ is known, $\hat{d}$ can be computed from (2.4.1) and the remaining cross-sectional properties from (2.2.29) and (2.2.30). Critical states are found by taking $\partial\mathcal{G}/\partial\overline{d} = 0$, resulting in

[1] It is not necessary that D_∞ be uniform from one fluid column to the next, only that D_∞ for each column be much larger than D. Thus the potential vorticity in the reservoir need not be uniform.

$$Q = \overline{d}_c^{\,3/2} w\,, \tag{2.4.4}$$

where the subscript c denotes a critical value. From (2.4.1) it follows that $2\hat{d}_c / w = \overline{d}_c^{\,1/2}$, or

$$\overline{v}_c = \overline{d}_c^{\,1/2}\,, \tag{2.4.5}$$

in view of the relation $2\hat{d} / w = \overline{v}$ derived in Section 2.2. As expected, Gill's criterion for critical flow matches the direct propagation speed calculation (2.2.31).

Possible locations where critical flow can occur are found by taking $[\partial \mathcal{G} / \partial y]_{\overline{d}=const.} = 0$, which leads to

$$\left(\frac{w}{4} - \frac{Q^2}{\overline{d}_c^{\,2} w^3} \right) \frac{\partial w}{\partial y} + \frac{\partial h}{\partial y} = 0\,. \tag{2.4.6}$$

In the WLK model w is constant and critical flow therefore requires that $\partial h / \partial y = 0$, as at a sill. In a channel of constant elevation h and variable w, critical flow requires that either $\partial w / \partial y = 0$, as at a narrows, or that the expression in parenthesis vanish. In the latter case (2.4.1) and (2.4.4) imply separation of the flow from the left wall ($\overline{d}_c = \hat{d}_c$). However this possibility can be eliminated, as explored in Exercise 1 of this section.

It is possible to obtain a 'weir' formula relating Q to the reservoir conditions. In the nonrotating example of Section 1.4 the formula was obtained by equating the Bernoulli functions at the sill and reservoir. Following the same procedure, we use (2.4.4) to evaluate (2.4.3) at the sill, leading to

$$\frac{3}{2}\left(\frac{Q}{w} \right)^{2/3} + \frac{w^2}{8} = \overline{B} - h_m\,, \tag{2.4.7}$$

where h_m is the sill elevation. Next, we need to evaluate $\overline{B}$ in the quiescent reservoir, being careful to avoid using the definition (2.4.2), which is not valid there. Instead we simply note, from primitive definition, that the Bernoulli function must be

$$B = D_\infty + h_\infty \tag{2.4.8}$$

where h_∞ is the reservoir bottom elevation. Since B is uniform throughout the reservoir, $\overline{B} = B$ and therefore

$$\frac{3}{2}\left(\frac{Q}{w} \right)^{2/3} + \frac{w^2}{8} = \Delta z \tag{2.4.9}$$

where $\Delta z = D_\infty + h_\infty - h_m$ is the elevation of the reservoir surface (or interface) above the channel bottom at the critical section. Rearranging (2.4.9) and writing the result in dimensional form gives

$$Q^* = \left(\frac{2}{3}\right)^{3/2} w^* g^{1/2} \left[\Delta z^* - \frac{w^{*2} f^2}{8g}\right]^{3/2} . \qquad (2.4.10)$$

As $f \to 0$ the limit (1.4.12) for nonrotating flow from a deep reservoir is realized. The reader is reminded that *g* represents either the full or reduced gravity, depending on whether the upper surface is interpreted as a free surface or deep interface.

If the flow in the channel becomes separated, we switch to the natural variables v_e and w_e (see Figure 2.3.1). The *y*-structure of the flow is then described by the steady forms of (2.3.16) and (2.3.17):

$$\tfrac{1}{2} w_e^2 (v_e - \tfrac{1}{2} w_e)^2 = Q \qquad (2.4.11)$$

and

$$\frac{v_e^{\,2}}{2} + h = \overline{B} . \qquad (2.4.12)$$

Note that the channel width *w* does not enter these relations. Changes in the position of the right-hand wall cause lateral displacements of the entire flow with no change in the shape of the interface.

Equation (2.4.12) expresses energy conservation along the free edge of the separated current. Since the depth is zero there, changes in the kinetic energy of the flow must be directly balanced by changes in bottom elevation. It is tempting to treat the left-hand side of this equation as a Gill-type hydraulic function $\mathcal{G}(v_e;h)$ since it contains the single flow variable v_e. However, taking $\partial \mathcal{G} / \partial v_e = 0$ results in v_e=0, whereas the true critical condition (see 2.3.18) based on wave speed calculation is v_e=w_e. On the other hand, one can use the multivariate critical condition:

$$\frac{\partial \mathcal{G}_1}{\partial w_w}\frac{\partial \mathcal{G}_2}{\partial v_e} - \frac{\partial \mathcal{G}_1}{\partial v_e}\frac{\partial \mathcal{G}_2}{\partial w_e} = 0 , \qquad (2.4.13)$$

based on (1.5.9). With $\mathcal{G}_1$ and $\mathcal{G}_2$ given by the left-hand sides of (2.4.11) and (2.4.12), this condition leads to the desired result

$$v_{ec} = w_{ec} . \qquad (2.4.14)$$

It is left as an exercise to show that the multivariate regularity condition (1.5.11) leads to the condition that $dh/dy = 0$ at a critical section.

The failure of the criterion $\partial \mathcal{G} / \partial v_e = 0$ to yield the correct critical condition in its application to (2.4.12) is tied into the peculiar dynamics of the frontal wave and the choice of v_e as the dependent variable. Consider the depth profile under critical conditions, as shown by the solid curve in Figure 2.4.1. The slope of the free surface is zero at the wall and v_e=w_e. Suppose that the profile is slid an infinitesimal distance to the right or left without changing its shape, as suggested by the dashed line. Since $\partial d / \partial x = 0$ at the wall the altered flow has the same wall depth, and therefore the same volume flux, as before. In addition the sideways displacement does not alter the value of B at the free edge, since v_e is unchanged. Since B is uniform when q=0, the value of $\bar{B}$ remains unchanged as well. In summary neither $\bar{B}$ nor Q is altered by the sideways displacement and the disturbance, which involves only changes in w_e, qualifies as a stationary long wave. [2] The condition $\partial \mathcal{G} / \partial v_e = 0$, which checks for disturbances in v_e that leave $\mathcal{G}$ unchanged, therefore misses the critical condition. In essence, satisfaction of Gill's criterion for a $\mathcal{G}$ written in terms of a particular dependent variable is a sufficient, but not necessary, condition for criticality. To avoid such cases one must be sure to use *all* the constraints available in the formulation. The multivariate version (1.5.14) of the critical condition therefore provides the safest route.

The weir formula for this case may be obtained using a similar procedure as above, resulting in

$$Q^* = \frac{g(\Delta z^*)^2}{2f} \tag{2.4.15}$$

for the separated case.

Equation (2.4.14) suggests that the separation first occurs at the critical section when $w_c = v_{ec}$ or, in view of (2.4.5), when $w_c = 2\bar{d}_c^{1/2}$. Furthermore, since v=0 at the right wall in this case, energy conservation implies that the level of the interface at the right wall is the same as that of the reservoir, so that $2\bar{d}_c = \Delta z$. Elimination of $\bar{d}_c$ between these last conditions leads to $\Delta z = w_c^2 / 2$, and therefore

$$w_c^* \begin{cases} < \sqrt{2}(g\Delta z^*)^{1/2}/f & \text{(non-separated)} \\ > \sqrt{2}(g\Delta z^*)^{1/2}/f & \text{(separated)} \end{cases} \tag{2.4.16}$$

That is, the flow at the critical section is separated if the channel width is greater than √2 times the Rossby Radius of deformation based on Δz^*. Thus, a decrease in reservoir surface elevation relative to the sill encourages critical separation of the flow.

---

[2] It should also be noted that the same argument is applicable to a separated flow with an arbitrary potential vorticity distribution. Such a flow is hydraulically critical if the velocity at the right wall vanishes.

WLK carried out an experiment designed to test the transport relations (2.4.10 and 2.4.15) and the separation criterion (2.4.16). Shen (1981) conducted further experiments using the same type of apparatus, which consists of a cylindrical tank divided into two basins by a vertical wall (Figure 2.4.2). Well above the bottom, a short channel with rectangular cross-section is fit through an opening in the wall. An alcohol-water mixture is filled up to the level of the bottom of the channel in both basins, and above this lies a layer of kerosene with slightly lower density. A pump transfers the lower fluid from the left-hand basin to the right, where it wells up through a packed bed of rocks. This fluid rises, passes through the channel, and spills into the right-hand basin. Photos of the overflow as seen looking upstream into the channel as well as from above appear in Figure 2.4.3. For the cases shown, the flow in the channel is non-separated, even though separation from the right wall (looking upstream) is predicted. The height Δz^* of the upstream interface above the channel bottom is measured by an optical device. The value of Q^* is measured directly by Shen, but not by WLK

The experiment is initiated by establishing a hydraulically controlled flow with f=0 and measuring the corresponding $\Delta z^*=\Delta z_o^*$. In principle, Δz_o^* should equal $\frac{3}{2} Q^{*2/3} g^{-1/3} w^{*-2/3}$. The turntable is then spun up to a particular f and, once a new steady state had been established, a new Δz^* is measured. The transport Q^* is determined only by the pumping rate and remains constant throughout the spin-up, so that the reservoir interface elevation is forced to adjust to drive the same amount of fluid across the sill.

For attached flow, the ratio $\Delta z^*/\Delta z_o^*$ can be determined using (2.4.9). The dimensional version of the result is

$$\frac{\Delta z^*}{\Delta z_o^*} = \frac{f^2 w^{*2}}{8 g \Delta z_o^*} + 1 . \qquad (2.4.17)$$

For the separated sill flow, the value of Δz^* is given by (2.4.15) and thus

$$\frac{\Delta z^*}{\Delta z_o^*} = \left(\frac{2}{3}\right)^{3/4} \left(\frac{4 w^{*2} f^2}{g \Delta z_o^*}\right)^{1/4} . \qquad (2.4.18)$$

The transition between the two cases occurs when $w^* = w_e^* = (2 g \Delta z^* / f^2)^{1/2}$, which corresponds to $\frac{3 w^{*2} f^2}{8 g \Delta z_o^2} = 1$ or $\frac{\Delta z^*}{\Delta z_o^*} = \frac{4}{3}$. A plot of the relation between $\frac{\Delta z^*}{\Delta z_o^*}$ and $\left[3 w^{*2} f^2 / 8 g \Delta z_o^*\right]^{1/2}$ along with the experimental data from WLK and Shen (1981) shows good agreement to the left of the transition (Figure 2.4.4). The data and theory in

this region agree to within 5%. To the right of the transition the agreement is within 20%. However, there was no clear evidence of separation in either experiment.[3]
Although the transport formulas (2.4.10) and (2.4.15) suggest that increasing f leads to smaller Q^*, this conclusion is only valid if the upstream interface level remains fixed. In reality, the effect of rotation on transport depends on how the flow is driven; in the WLK experiment Q^* is maintained at a fixed rate while f is varied.

Shen (1981) also investigated flows that remain subcritical over the entire domain and are therefore not hydraulically controlled. Transport relations like (2.4.10) and (2.4.15) are clearly no longer valid for such flows and one may ask whether there is another strategy for measuring the volume flux. The chief obstacle is that the critical condition over the controlling weir or sill is lost and the flow is therefore less constrained. Civil engineers encounter this problem when a weir that normally produces a subcritical-to-supercritical transition becomes 'submerged', meaning that the transition region has become flooded and subcritical.

According to our inviscid models, is no difference between the surface heights of a subcritical flow upstream and downstream of an isolated obstacle (Figure 2.4.5). In reality, the surface level always drops slightly due to a frictional energy loss over the obstacle. Real world flows also tend separates from the channel sidewalls and/or the bottom, if broadening of the channel downstream of the contraction or sill is abrupt. In the case of sidewall separation, pools containing weak recirculations exist along the side-walls of the flow. These features also enhance the asymmetry between the upstream and downstream. One strategy for measuring the volume flux of such a flow is to measure the upstream and downstream surface elevations and relate Q to their difference.

Shen describes a procedure along these lines for a rotating, subcritical flow with uniform potential vorticity. He assumes that separation occurs from the left wall of the channel as the subcritical flow passes the most constricted section. (The constriction in his experiment takes the form of a uniform length of channel separating two deep reservoirs, as in Figure 2.4.2.) The geostrophic flux in the channel is given by $Q^* = \frac{g}{2f}\left(d^{*2}_R - d^{*2}_L\right)$, where d^*_R and d^*_L are right and left wall depths. A key assumption is that the downstream separation causes the surface elevation along the left wall to be nearly equal to that downstream of the channel and in the stagnant pool on the left wall. Thus $d^*_L = D_{-\infty} - h_m^*$, where $D_{-\infty}$ is the downstream depth in the pool and h_m^* is the elevation of the channel bottom relative to the downstream bottom. Also d^*_R can be related to the upstream interior depth D_∞ using constraints provided by the Bernoulli function, which is assumed to be conserved in the upstream region, and the assumption of uniform potential vorticity. In this way Q^* is related to D_∞ and $D_{-\infty}$. Computation of the volume flux therefore requires two depth measurements in quiescent areas, one upstream

[3] If fact, more recent laboratory and numerical experiments have largely failed to produce flow separation. We will mention many of these experiments throughout the remainder of the book.

and the other downstream of the sill or channel. The reader should consult Shen's (1981) paper for the formulae, which are quite involved.

Shen carried out laboratory experiments to test the submerged weir theory in the limit of zero potential vorticity (Figure 2.4.6). One complicating factor is that some of the solutions exhibit flow reversal ($v<0$) along the right wall of the channel. In such cases, the predicted flux is based only on that part of the flow with $v>0$. The possible flow regimes include critical flow without reversal (I); submerged flow without reversal (II); submerged flow with reversal (III); and critical flow with reversal (IV). As indicated by the crosses in the figure, there are few observations of flow in regime III. The theory, which is represented by four curves for four channel widths, relates the upstream level Δz of the interface (relative to the channel bottom) to a nondimensional flux Q'. The dependence on the downstream flow is hidden in the scaling factor $D = \frac{1}{2}\left(D_{\infty} + D_{-\infty} - 2h_m^*\right)$, which is used in the nondimensionalization. It is evident that the agreement between theory and experiment is quite good for the cases shown. It is not known how accurate the formulae are for other geometries or separation scenarios.

The experiments of WLK and of Shen (1981) were designed to approximate the zero potential vorticity limit by causing fluid to be drawn from a deep, quiescent reservoir. Clearly, the long wave approximation is violated at the entrance of the channel, where an abrupt change in geometry occurs. Also, a gyre generally forms in the deep upstream fluid, making the assumption of quiescence doubtful. Despite the violations of underlying assumptions, agreement between predicted and observed transports is generally good. In fact the models of WLK and Shen some of the very few that have been subjected to careful laboratory verification. As we will show in Section 2.6, the relation (2.4.15) provides the transport under more general conditions, provided Δz^* is suitably interpreted. It will also be shown (Section 2.10) that the same relation provides a bound on the transport in even more general circumstances.

Exercises

1) Consider a channel with variable w and constant h. Equation (2.4.6) suggests that a critical section in such a channel can occur where $\partial w / \partial y = 0$ or where $w^2 = 2Q / \bar{d}_c$.

(a) Show that the latter implies $\bar{d}_c = \hat{d}_c$ (the flow is separating from the left wall).

(b) Suppose that separation occurs at a section $y=y_s$ where the width is changing and suppose, with no loss in generality, that $dw/dy>0$. Now consider a section slightly upstream of $y=y_s$, where the flow is attached. Show by conservation of Q that the right wall depth at the upstream section must be greater than that at y_s. Using the fact that the right-wall velocity at y_s must be zero, show that the value of the right-wall Bernoulli function cannot be conserved between the two sections and therefore a continuous solution is not possible.

2) Suppose that the channel draining the reservoir in the WLK model has constant w. Further suppose that the flow separates from the left wall upstream of the sill. Given the values of w, h_m, and Δz, at what value of h does separation occur?

3) Equations (2.4.11) and (2.4.12) can be cast as two hydraulic functions $\mathcal{G}_1$ and $\mathcal{G}_2$ in the two variable space (w_e, v_e). Show that the stationary wave displacement vector defined by (1.5.10) is aligned in the direction (1,0). Can you use this result to explain the failure of the (2.4.12), when treated as a single function in the single variable v_e, to provide the correct critical condition?

Figure Captions

Figure 2.4.1 Cross section (surface profile) of a critical, separated current (solid curve) and a new steady flow with the same Bernoulli function and volume flux, created by a sideways displacement of the current (dashed line).

Figure 2.4.2 Cross section of the cylindrical tank used in the WLK experiments. (From Whitehead et al. 1974).

Figure 2.4.3 Top view (column A) and front view (column B) of overflow through a rectangular channel. The ends are flared to permit smoother flow. Rotation rate is progressively greater starting from zero in rows 1-5, so $\sqrt{2g\Delta z^*}/wf$ takes the following values ∞, 3.0, 1.57, 0.75, and 0.68. (From Shen, 1981).

Figure 2.4.4 Comparison of the WLK theory (curves given by equations 2.4.17 and 2.4.18), with experimental data from WLK (circles with error bars) and Shen (crosses denoting error bars). (Adapted from Whitehead et al. 1974 and Shen, 1981).

Figure 2.4.5 The top frame shows the surface profile for an idealized subcritical flow with no friction and the modification (dashed extension) caused by frictional effects, possibly associated with flow separation downstream of the sill. The lower curve shows a hydraulically controlled flow with a jump. The lower frame shows sidewall separation and the closed gyres with weak circulation that can be produced as a consequence.

Figure 2.4.6 Transport $Q' = Q/Q_c$ versus the dimensionless upstream elevation $\Delta z=\Delta z^*/D$ above the sill for various channel widths $w=w^*f/(gD)^{1/2}$. Downstream information is contained in the scale factor $D=\frac{1}{2}(D_\infty+D_{-\infty}-2h_m^*)$. Q_c refers to the flux that occurs for the same value of w at the point where the flow is marginally submerged. The solid curves correspond to the equations appearing in Table 1 of Shen (1981). The dashed lines are the boundaries of the four regimes (I) critical flow without reversal, (II) Submerged flow without reversal, (III) Submerged flow with reversal, and (IV) critical flow with reversal. The bars denote the measurements and their uncertainty. (From Shen, 1981).

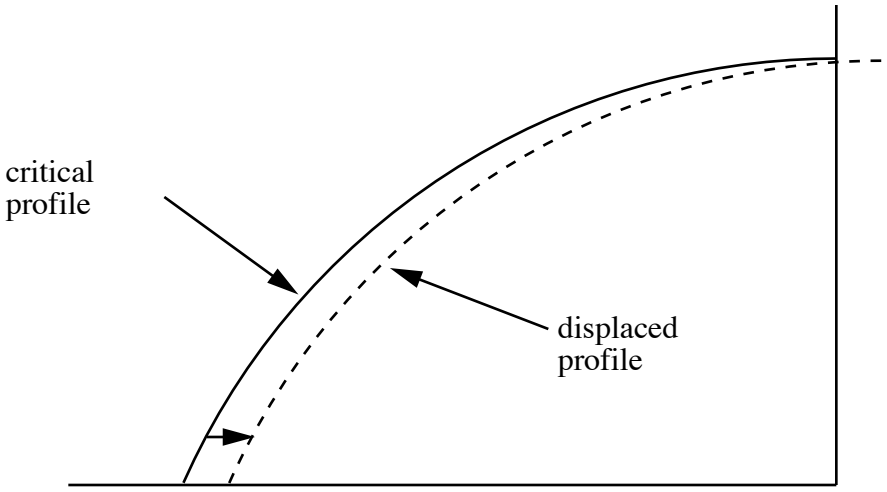

Figure 2.4.1

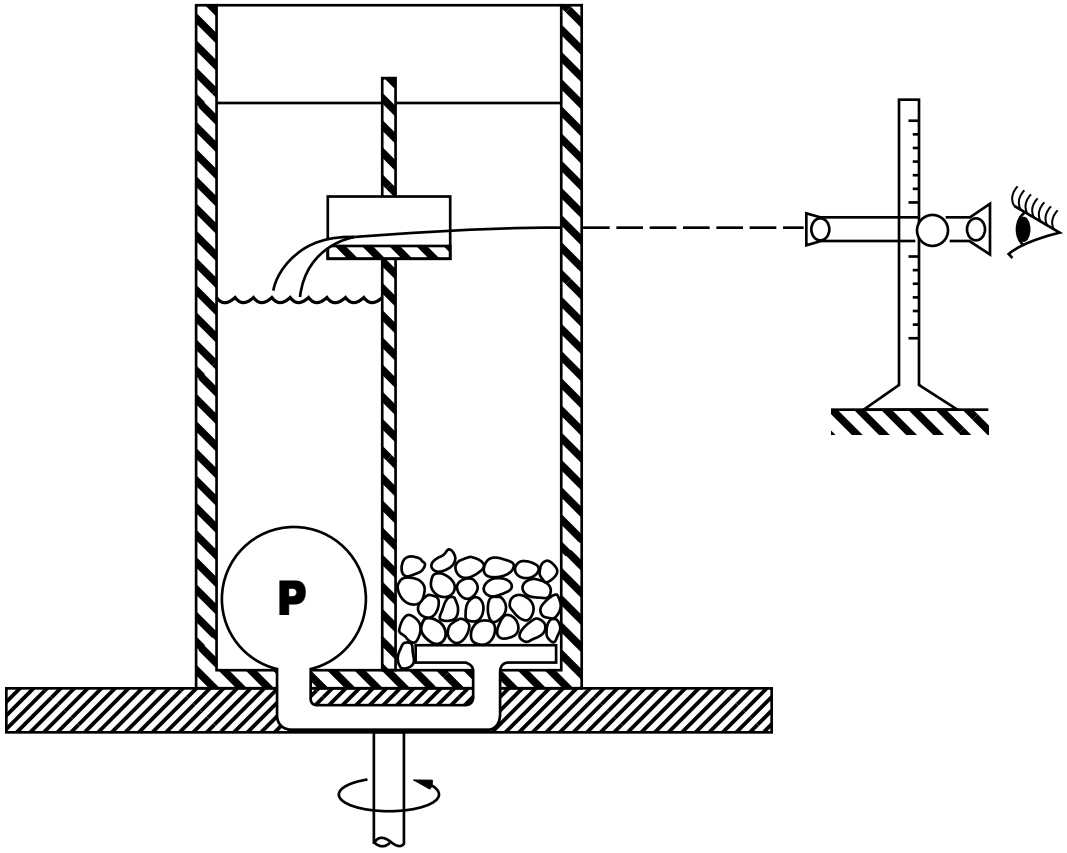

Figure 2.4.2

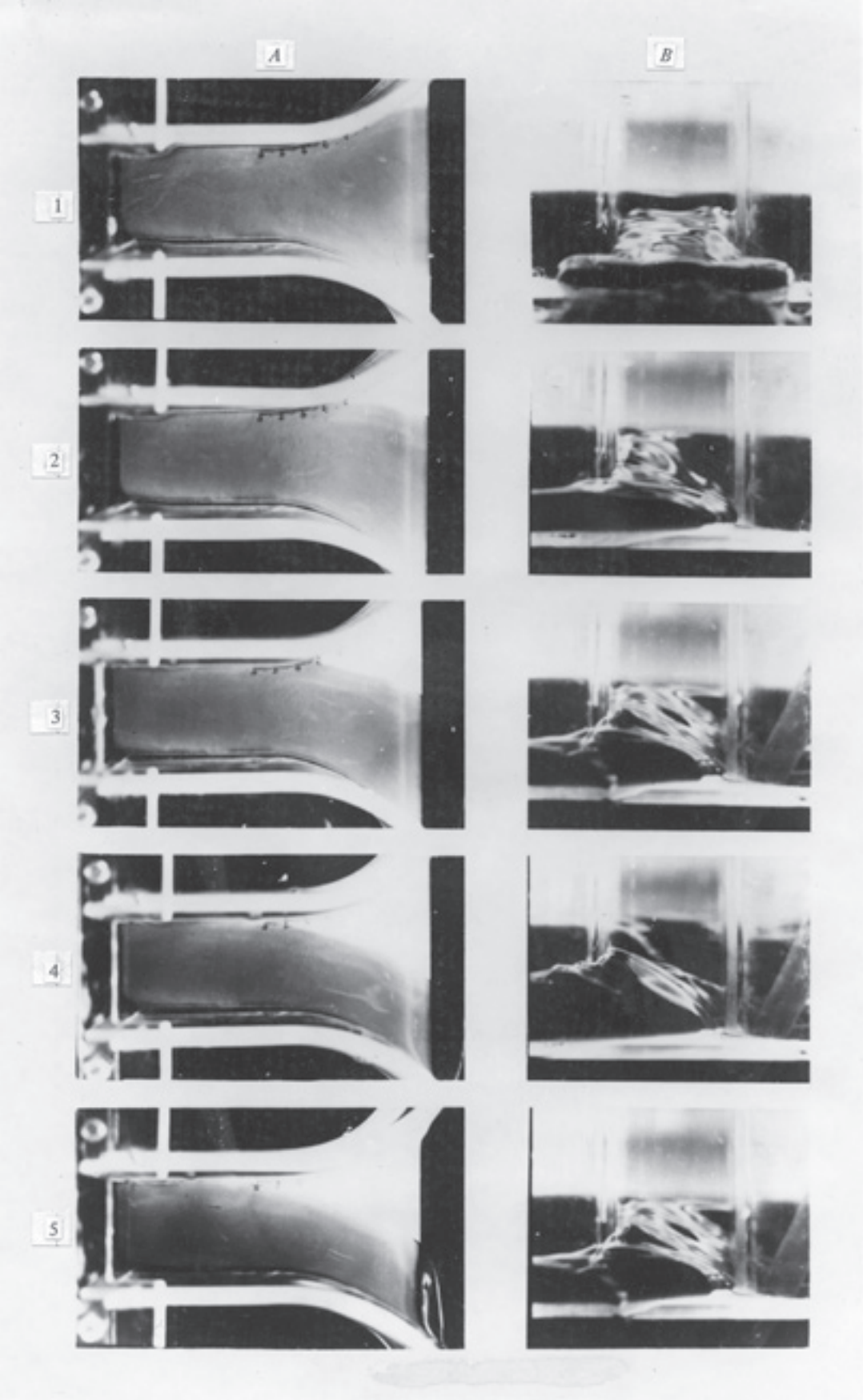

Figure 2.4.3 low resolution ver.

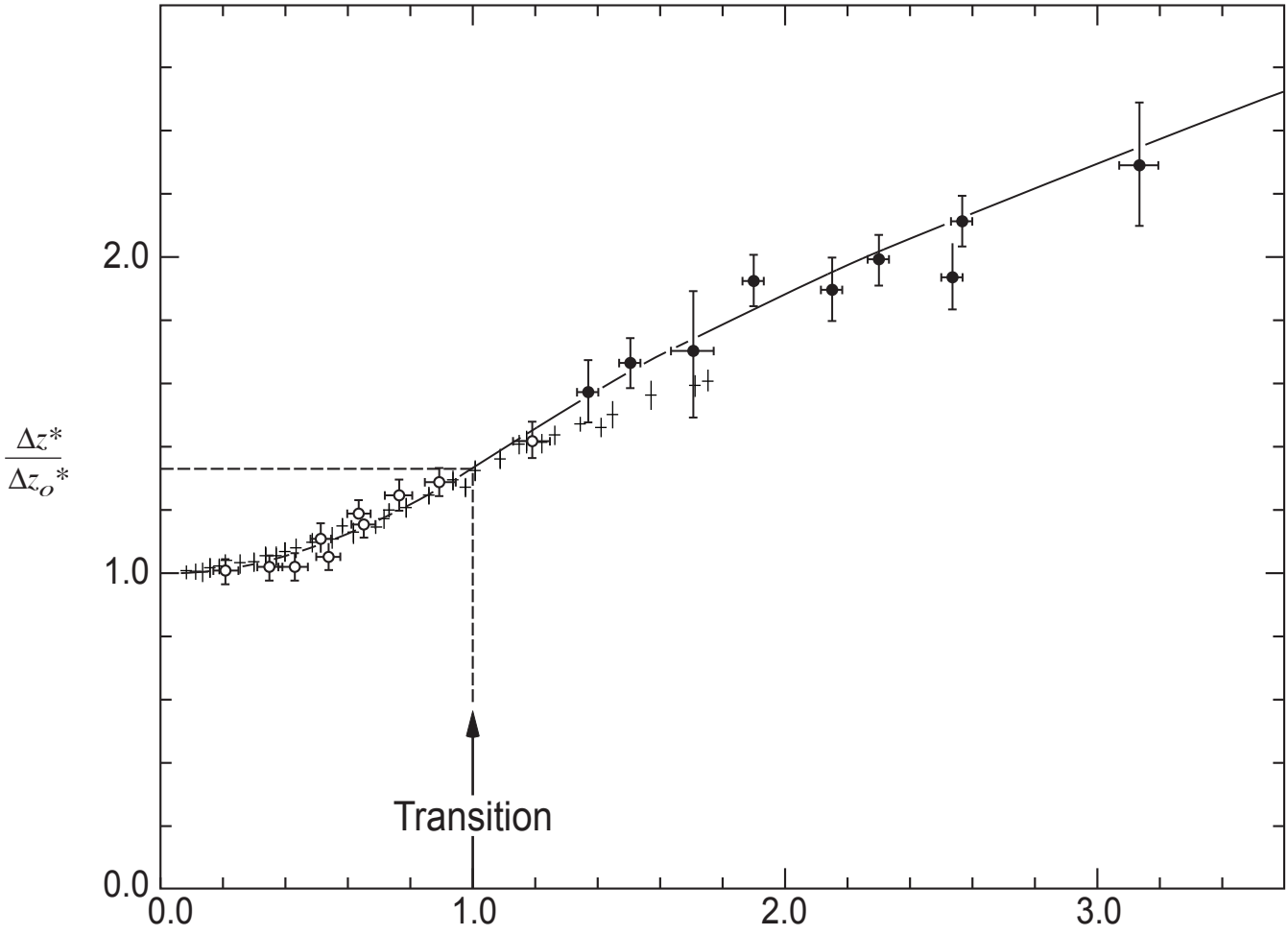
$\frac{\Delta z^*}{\Delta z_o^*}$
2.0
1.0
0.0
0.0
1.0
2.0
3.0
Transition
$[3w^{*2}f^2/8g'\Delta z_o^*]^{1/2}$

Fig. 2.4.4

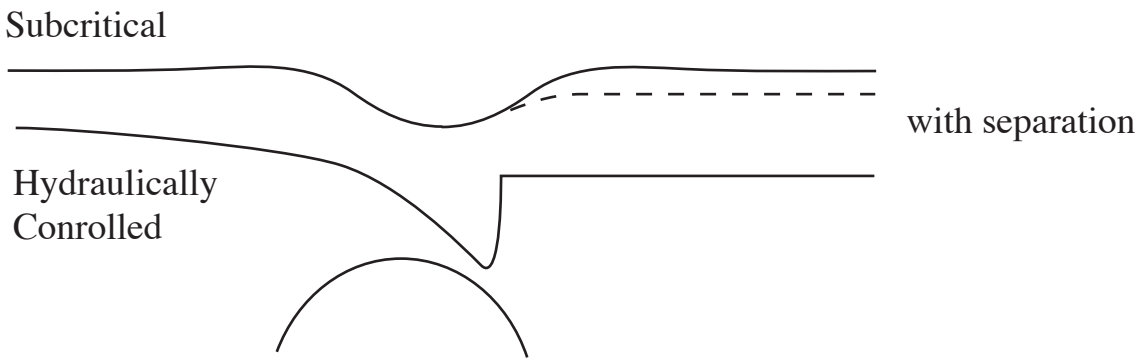
Subcritical
with separation
Hydraulically
Conrolled

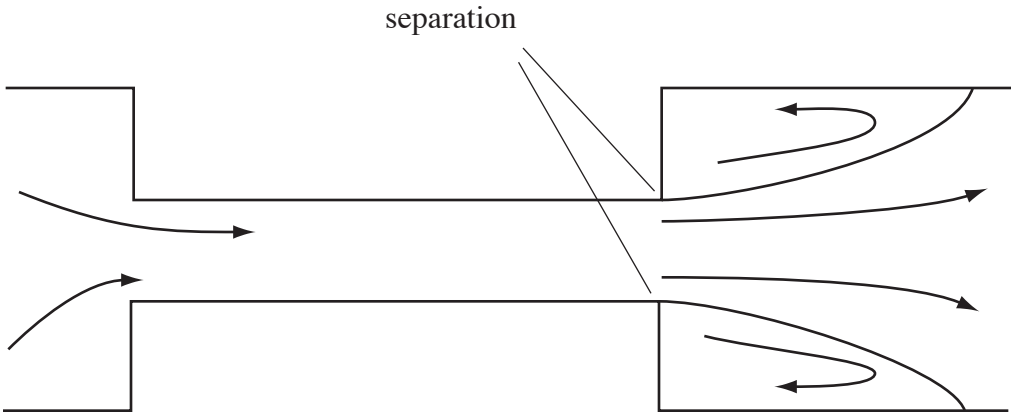
separation

Figure 2.4.5

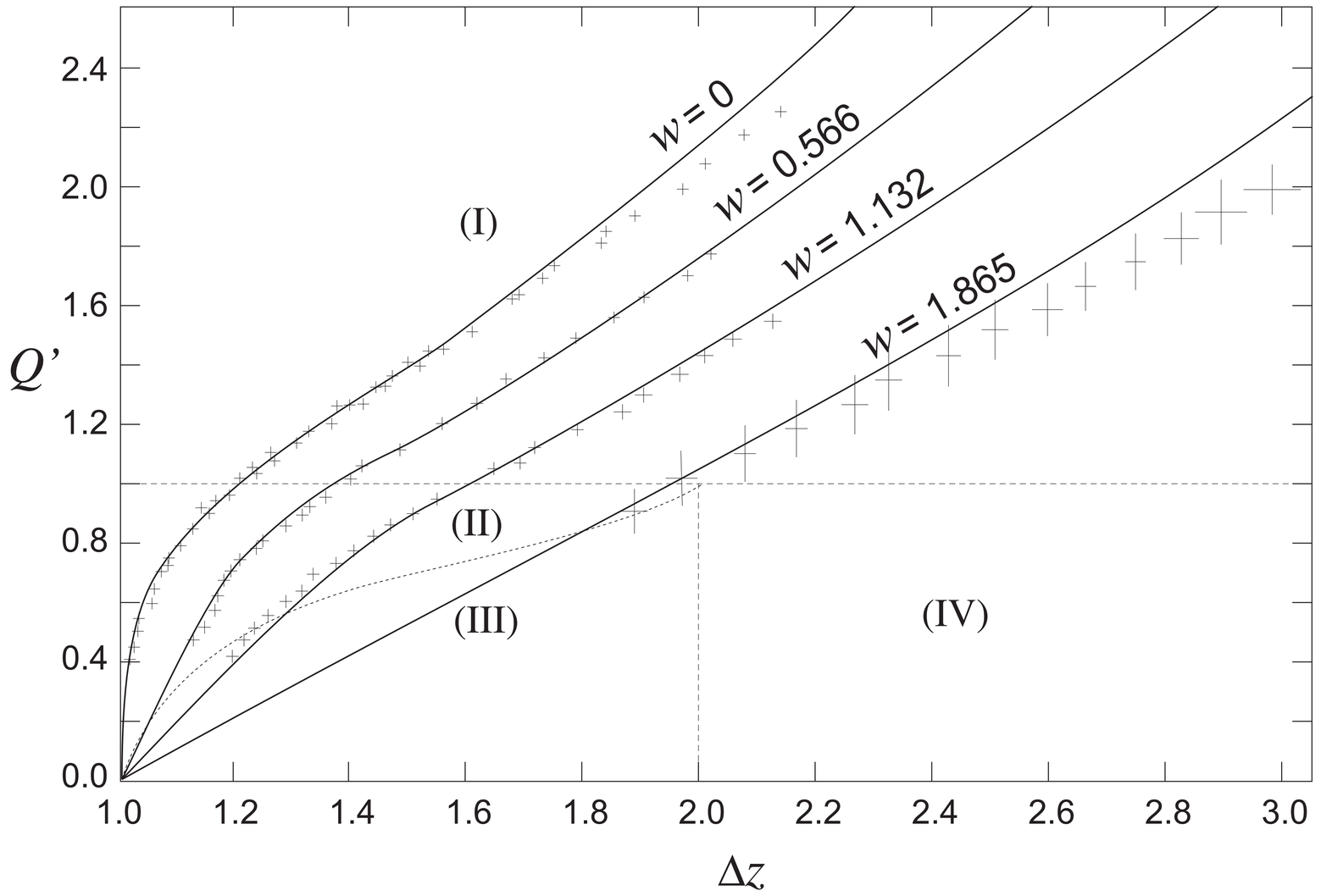
2.4
2.0
1.6
1.2
0.8
0.4
0.0
Q'
w = 0
w = 0.566
w = 1.132
w = 1.865
(I)
(II)
(III)
(IV)
1.0
1.2
1.4
1.6
1.8
2.0
2.2
2.4
2.6
2.8
3.0
Δz

Fig. 2.4.6